Antimicrobial sensing coupled with cell membrane remodeling mediates antibiotic resistance and virulence in *Enterococcus faecalis*

Ayesha Khan[a,b,c,d], Milya Davlieva[e], Diana Panesso[a,b,f], Sandra Rincon[f], William R. Miller[a,b], Lorena Diaz[f,g], Jinnethe Reyes[f], Melissa R. Cruz[c], Orville Pemberton[e], April H. Nguyen[a,b,c,d], Sara D. Siegel[c], Paul J. Planet[h,i,j], Apurva Narechania[j], Mauricio Latorre[k,l,m], Rafael Rios[f], Kavindra V. Singh[a,b], Hung Ton-That[n], Danielle A. Garsin[a,c,d], Truc T. Tran[a,b], Yousif Shamoo[e], and Cesar A. Arias[a,b,c,d,f,o,1]

[a]Center for Antimicrobial Resistance and Microbial Genomics, McGovern Medical School, University of Texas Health Science Center, Houston, TX 77030; [b]Division of Infectious Diseases, McGovern Medical School, University of Texas Health Science Center, Houston, TX 77030; [c]Department of Microbiology and Molecular Genetics, McGovern Medical School, University of Texas Health Science Center, Houston, TX 77030; [d]MD Anderson Cancer Center, University of Texas Health Graduate School of Biomedical Sciences, Houston, TX 77030; [e]Department of Biosciences, Rice University, Houston, TX 77005; [f]Molecular Genetics and Antimicrobial Resistance Unit, International Center for Microbial Genomics, Universidad El Bosque, 110111 Bogotá, Colombia; [g]Millennium Initiative for Collaborative Research On Bacterial Resistance (MICROB-R), 8320000 Santiago, Chile; [h]Perelman School of Medicine, University of Pennsylvania, Philadelphia, PA 19104; [i]Pediatric Infectious Disease Division, Children's Hospital of Philadelphia, Philadelphia, PA; [j]Sackler Institute for Comparative Genomics, American Museum of Natural History, New York, NY 12560; [k]Center for Genome Regulation and Center for Mathematical Modeling, Universidad de Chile, 8320000 Santiago, Chile; [l]Laboratorio de Bioinformática y Expresión Génica, Instituto de Nutrición y Tecnología de los Alimentos, Universidad de Chile, 8320000 Santiago, Chile; [m]Laboratorio de Biotecnología, Instituto de Ciencias de la Ingeniería, Universidad de O'Higgins, 2841158 Rancagua, Chile; [n]Division of Oral Biology and Medicine, School of Dentistry, University of California, Los Angeles, CA 90024; and [o]Center for Infectious Diseases, School of Public Health, University of Texas Health Science Center, Houston, TX 77030

Bacteria have developed several evolutionary strategies to protect their cell membranes (CMs) from the attack of antibiotics and antimicrobial peptides (AMPs) produced by the innate immune system, including remodeling of phospholipid content and localization. Multidrug-resistant *Enterococcus faecalis,* an opportunistic human pathogen, evolves resistance to the lipopeptide daptomycin and AMPs by diverting the antibiotic away from critical septal targets using CM anionic phospholipid redistribution. The LiaFSR stress response system regulates this CM remodeling via the LiaR response regulator by a previously unknown mechanism. Here, we characterize a LiaR-regulated protein, LiaX, that senses daptomycin or AMPs and triggers protective CM remodeling. LiaX is surface exposed, and in daptomycin-resistant clinical strains, both LiaX and the N-terminal domain alone are released into the extracellular milieu. The N-terminal domain of LiaX binds daptomycin and AMPs (such as human LL-37) and functions as an extracellular sentinel that activates the cell envelope stress response. The C-terminal domain of LiaX plays a role in inhibiting the LiaFSR system, and when this domain is absent, it leads to activation of anionic phospholipid redistribution. Strains that exhibit LiaX-mediated CM remodeling and AMP resistance show enhanced virulence in the *Caenorhabditis elegans* model, an effect that is abolished in animals lacking an innate immune pathway crucial for producing AMPs. In conclusion, we report a mechanism of antibiotic and AMP resistance that couples bacterial stress sensing to major changes in CM architecture, ultimately also affecting host–pathogen interactions.

antibiotic resistance | *Enterococcus faecalis* | daptomycin | cell membrane adaptation | antimicrobial peptides

Antibiotic resistance has been recognized as a major global health threat of the 21st century (1). Vancomycin-resistant enterococci (VRE) are among the most challenging organisms to treat, as some display resistance to all available antimicrobials used in clinical practice (2). Enterococci evolved resistance under the selective pressures of the modern health care environment due to their genomic plasticity and ability to acquire and disseminate a wide repertoire of antibiotic resistance determinants (3).

Daptomycin (DAP) is a frontline antibiotic against deep-seated VRE infections (4); however, the emergence of daptomycin resistance (DAP-R) in clinical settings emphasizes the need for novel therapies (5). DAP is a cell membrane (CM)-acting, cationic

antibiotic that targets anionic phospholipids at the bacterial division septum (6). DAP insertion into the CM (6) leads to mislocalization of membrane proteins involved in maintaining cell envelope homeostasis, leading to cell death (7). Similarly, cationic

Significance

Vancomycin-resistant enterococci are hospital-associated pathogens that evolved resistance to most antibiotics used in clinical practice. Daptomycin, a lipopeptide antibiotic used as frontline therapy for severe multidrug-resistant enterococcal infections, targets the bacterial cell membrane (CM). The LiaFSR stress response system orchestrates daptomycin and antimicrobial peptide (AMP) resistance by modulating CM phospholipid content or localization. Here, we identify a single protein (LiaX) that senses antimicrobial molecules and regulates changes in CM phospholipid architecture. We show that LiaX-mediated modulation of antibiotic and AMP resistance affects virulence during infection caused by a recalcitrant hospital pathogen. Targeting this response in multidrug-resistant organisms may be a therapeutic intervention to restore susceptibility to cell envelope-targeting antibiotics and increase the ability of the immune system to clear pathogens.

MICROBIOLOGY

antimicrobial peptides (AMPs) produced by the innate immune system exert their antibacterial activity through CM disruption (8, 9).

Emergence of DAP-R in clinical and laboratory settings is described in *Enterococcus faecalis* and *Enterococcus faecium* (5). In *E. faecalis*, DAP-R is associated with changes in CM phospholipid composition (10) and redistribution of anionic phospholipids away from the septum, diverting DAP (11, 12). These changes are linked to mutations in genes encoding the LiaFSR system and enzymes involved in phospholipid metabolism (13). LiaFSR (for lipid-II–interacting antibiotics) is a 3-component stress response system conserved across *Firmicutes* that regulates cell envelope integrity (14). A deletion of the gene encoding the LiaR response regulator leads to hypersusceptibility to DAP and AMPs (15). *E. faecalis* lacking LiaR is more susceptible to killing by innate immune cells (16). Quantitative experimental evolution has shown that pathways to DAP-R require initial activation of the LiaFSR response followed by changes in phospholipid enzymes (17). However, the mechanism by which LiaR affects cell envelope integrity on exposure to antibiotics and AMPs is unknown.

Here, we identify the genetic and biochemical basis of the adaptive response to CM active antibiotics in *E. faecalis*. We characterize LiaX, a protein of previously unknown function, as the main mediator of the LiaR-directed CM response to DAP and AMPs. Each domain of LiaX plays a unique function in modulating DAP-R. The C-terminal domain of LiaX inhibits the LiaFSR system in wild-type strains. Thus, the absence of the C-terminal domain releases this inhibition and acts as a signal to trigger the CM stress response. The N-terminal domain functions as a sentinel that can bind DAP and AMPs in the extracellular environment, leading to activation of the LiaFSR system and protection against antimicrobials. DAP-R strains show enhanced virulence in vivo in a *Caenorhabditis elegans* infection model relative to daptomycin-susceptible (DAP-S) strains due to resistance to the innate immunity. Supplementing the *C. elegans* infection assay with the N-terminal domain of the LiaX is sufficient to enhance the virulence of DAP-S strains. Thus, LiaX functions as a modulator of the CM stress response linking membrane adaptation, antibiotic resistance, and pathogenesis.

Results

Determination of the LiaR Regulon. We hypothesized that the biochemical mechanism of DAP-R is mediated by genes regulated by the LiaFSR system. Thus, we used transcriptomics to identify target genes in the LiaR regulon. Genes mediating DAP-R were identified by comparing 1) a clinical strain pair of DAP-S and DAP-R *E. faecalis* (S613 and R712) recovered from the bloodstream of a patient before and after DAP therapy, respectively (13), and 2) a DAP-R derivative of S613 that harbors the mutated alleles from R712 [S613Δ$_{liaF177gdpD170cls61}$; referred herein as TM (13)] with its derivative that has a deletion of *liaR* and is hypersusceptible to DAP (12). We identified 3 proteins encoded by the *liaXYZ* operon (*SI Appendix*, Fig. S1) as well as genes coding for transmembrane proteins of unknown function and proteins involved in cell envelope stress responses, cell division, and cell wall synthesis among others (*SI Appendix*, Fig. S2 and Table S3). Previous structural studies showed that, on activation, LiaR oligomerizes, increasing its ability to bind regulatory DNA sequences upstream of *liaFSR* and *liaXYZ* and recruit RNA polymerase (18). Thus, we focused on *liaXYZ* and used qRT-PCR to verify them as potentially important effectors of LiaR (*SI Appendix*, Figs. S1 and S2 and Table S3).

The first gene of the *liaXYZ* cluster (*liaX*) encodes a 533-amino acid (AA) protein with 2 distinct predicted domains: an N-terminal domain composed mainly of α-helices and a C-terminal domain formed largely of β-strands (*SI Appendix*, Fig. S1). LiaX lacks predicted classical secretion signals, an LPXTG motif, and transmembrane domains. *liaY* encodes a 107-AA transmembrane protein harboring a PspC domain that is involved

in cell envelope stress adaptation in gram-negative bacteria (19). *liaZ* encodes a 118-AA transmembrane protein with homology to bacterial holins involved in the response to phage-mediated membrane damage (20).

The C-Terminal Domain of LiaX Regulates CM Adaptation. Experimental evolution of the DAP-S clinical isolate S613 identified that mutations in *liaF*, *liaS*, or a frameshift stop codon at predicted AA position 289 in LiaX were crucial in the initial adaptive trajectory to DAP-R (17). Position 289 is within a protease susceptible linker region that bridges the N- and C-terminal domains of LiaX, suggesting that a C-terminal domain truncation is important for adaptation to DAP. Thus, to verify the role of LiaX and the function of the C-terminal domain, we generated a nonpolar deletion of *liaX* (OG1RFΔ*liaX*) and truncation of the C-terminal domain (stop codon at AA 289, OG1RF$_{liaX*289}$) in a DAP-S laboratory strain of *E. faecalis* (OG1RF). Deletions of *liaX* and the C-terminal domain-encoding region made OG1RF resistant to DAP (8-fold increase in minimum inhibitory concentration [MIC]) with anionic phospholipids redistributed away from the division septum as evidenced by the pattern of 10-*N*-nonyl acridine orange staining (Fig. 1 and *SI Appendix*, Fig. S3). Complementation of *liaX* in the mutants reverted the resistance phenotype and reestablished septal localization of anionic phospholipids (Fig. 1 and *SI Appendix*, Fig. S3). Analysis of membrane composition of major lipids in exponential-phase cells showed an increase in phosphatidylglycerol (PG) and a decrease in cardiolipin in DAP-R laboratory (OG1RFΔ*liaX*, OG1RF$_{liaX*289}$) and clinical (R712) strains relative to their DAP-S counterparts, with no changes observed in lysyl-PG (*SI Appendix*, Fig. S4). Complementation of *liaX* (OG1RFΔ*liaX* pAT392::*liaX*) fully reverted this phenotype (*SI Appendix*, Fig. S4). Of note, these lipid composition changes differ from previous studies conducted on stationary-phase cells (10).

The deletion of *liaX* or its C-terminal domain led to the activation of the LiaFSR stress response system as indicated by the up-regulation of the *liaFSR* and *liaXYZ* gene clusters relative to the DAP-S, OG1RF (*SI Appendix*, Fig. S5). Thus, the C-terminal domain of LiaX acts as a negative regulator of the LiaFSR system, and in the absence of this domain, constitutive activation of the system leads to CM remodeling that modulates antibiotic resistance.

LiaX and Its N-Terminal Domain Are Released into the Extracellular Environment in DAP-R Strains. Since LiaX has 2 distinct domains, we hypothesized that the subcellular localization of LiaX is important for its function. Localization was probed with an enzyme-linked immunosorbent assay (ELISA) and immunoblotting on whole cells, cell wall or CM extracts, and concentrated supernatants using an affinity purified antibody to the N terminus of LiaX. All experiments were performed with pairs of DAP-R and DAP-S clinical and laboratory strains. The 60-kDa LiaX or the N terminus alone (∼30 kDa) was detected on the cell surface and extracellular milieu in significantly higher amounts in all DAP-R strains (clinical or laboratory origin) compared with the DAP-S parental strains (Fig. 2). Notably, the N-terminal domain of LiaX is detected along with full-length LiaX in the supernatants of the DAP-R clinical strains (Fig. 2*C*).

To identify changes in LiaX localization under antibiotic exposure, DAP-S and DAP-R strains were incubated with increasing DAP concentrations prior to immunoblotting. LiaX was detected in the whole-cell lysates and supernatants of DAP-S strains in a concentration-dependent manner, while DAP-R strains constitutively produced and released high amounts of LiaX (*SI Appendix*, Fig. S6). A band corresponding to the N terminus was also detected in strains that harbored the full-length *liaX* in the lysates or supernatants, indicating that LiaX is likely processed and that the N-terminal end is released
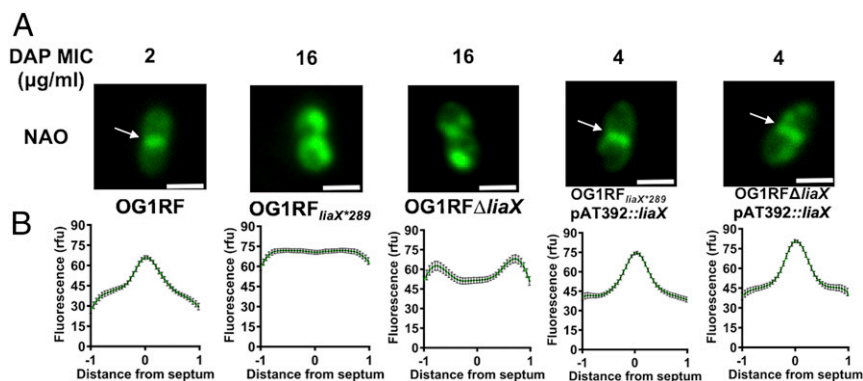
Fig. 1. LiaX regulates CM remodeling in *E. faecalis*. (*A*) Representative fluorescence microscope images of anionic phospholipids visualized in *E. faecalis* strains grown to midexponential phase by staining with 10-*N*-nonyl acridine orange (NAO). A nonpolar deletion (OG1RF∆*liaX*) and a C-terminal truncation (OG1RF*liaX*289*) lead to DAP-R as seen with the 8-fold increase in DAP MIC and a redistribution of anionic phospholipids away from the division septum (white arrow). (Scale bar: 0.5 µM.) (*B*) Mean fluorescence intensity (relative fluorescence units [rfu]) across cell length (represented on the *x* axis as a fraction of the distance from the midcell division septum) was quantified from 25 to 50 single cells for each strain, with error bars indicating the SD at each point in the cell.

separately. To determine if overproduction of LiaX is sufficient for extracellular secretion, we cloned *liaX* in plasmid pMSP3535 under a nisin-inducible promoter and delivered the construct to OG1RF∆*liaX*. Induction with ascending concentrations of nisin led to increased expression and eventual secretion of both full-

length and N-terminal LiaX (*SI Appendix*, Fig. S7). Additionally, we sought to visualize LiaX in the extracellular milieu using immunogold labeling and transmission electron microscopy. More LiaX was detected in the extracellular milieu of DAP-R compared with DAP-S strains (*SI Appendix*, Fig. S8). Our results
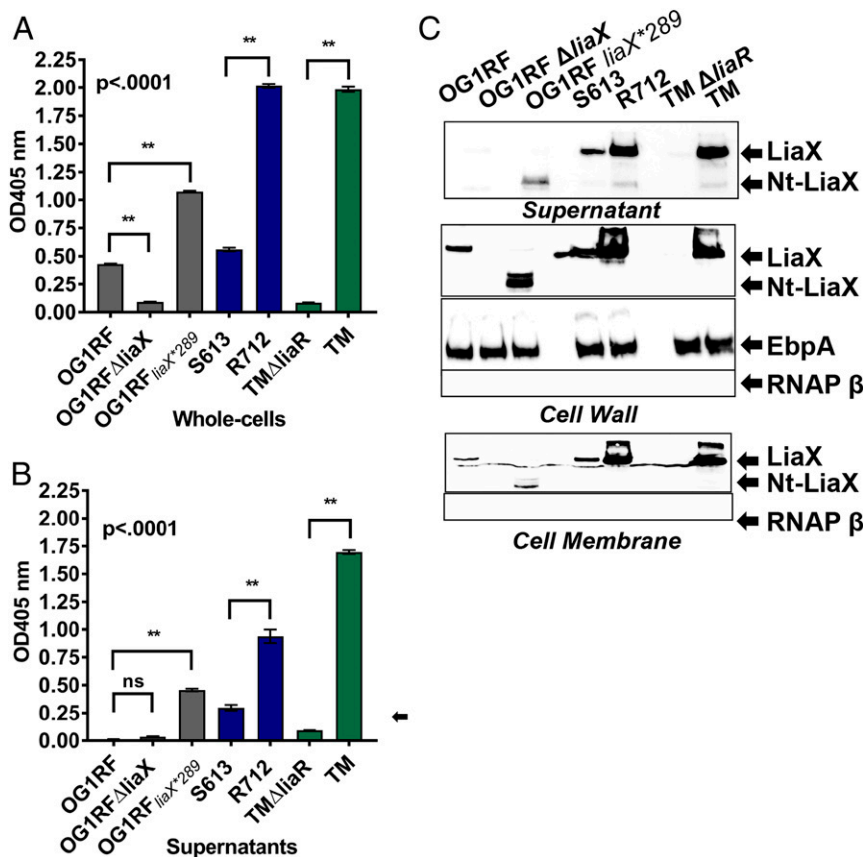

Fig. 2. LiaX is highly surface exposed and released into the extracellular environment in DAP-R strains. ELISA with optical density measured at a wavelength of 405 nm (OD405), using affinity purified antibody to the N-terminal domain of LiaX on the cell surface (*A*) and in TCA precipitated supernatants (*B*). OG1RF∆*liaX* was used as a negative control. All DAP-R strains have increased detection of LiaX compared with their DAP-S counterparts. Statistics display mean values from 3 independent experiments with 24 replicates each and error bars for SEM. ns, not significant. **$P < 0.0001$ (2-tailed *t* test). (*C*) Immunoblotting to detect LiaX full length (60 kDa; upper band) or N terminus (30 kDa; lower band) in the CM, cell wall, and supernatant fractions of DAP-S and DAP-R strains. Despite lacking identifiable transmembrane domains or LPXTG motifs, LiaX is seen in all fractions. EbpA, a cell surface pilli protein, was used as a cell wall loading control. RNA polymerase β-subunit (RNAP β), a cytosolic protein, was used as a quality control to ensure purity of the cell wall and membrane fractions.

indicate that development of DAP-R involving CM remodeling was associated with increased cell surface exposure and extracellular release of LiaX and/or the N terminus of the protein.

LiaX Binds DAP and the Human Cathelicidin LL-37. To dissect the extracellular role of LiaX, we postulated that LiaX could bind DAP or AMPs to "shield" the cell from the antibiotic attack. The human cathelicidin LL-37 (21) is a peptide secreted by polymorphonuclear leukocytes to disrupt the bacterial CM and is functionally similar to DAP. Enterococci lacking *liaR* are more susceptible to killing by human neutrophils, presumably by enhancing the ability of LL-37 to kill the invading bacteria (16). DAP-R has been associated with cross-resistance to AMPs, including LL-37 (22). In agreement with those studies, all laboratory and clinical DAP-R strains (including OG1RFΔ*liaX*) were resistant to LL-37 killing compared with their DAP-S counterparts (*SI Appendix*, Fig. S9). Furthermore, reintroduction of *liaX* in OG1RFΔ*liaX* reverted the resistance phenotype. We then tested the ability of both LiaX and the N-terminal domain to bind DAP using fluorescence spectroscopy. The disassociation constant (K_d) for the full LiaX protein was 30.4 ± 6.1 nM in the presence of 1 mM Ca^{+2}, while the N-terminal domain had a modestly lower affinity ($K_d = 83.8 \pm 6.6$ nM) (Fig. 3*A* and *SI Appendix*, Table S4). DAP MICs for enterococci range from ~0.25 to over 20 μg/mL (1.5 to 12 μM), which is more than 10 times our measured in vitro K_d levels. Thus, LiaX binding to DAP occurs within physiologically relevant concentrations. LL-37 binding to LiaX was measured using microscale thermophoresis (MST) by quantifying changes in fluorescence emitted by NT-647–labeled LiaX (Fig. 3*B*). The K_d for LiaX was 8.26 ± 0.28 μM, and it was 10.6 ± 0.43 μM for the N terminus of LiaX (*SI Appendix*, Table S4). There is a modest sigmoidal character to the binding isotherms, suggesting cooperativity during binding (Fig. 3*B*). The binding affinity of the N terminus of LiaX to LL-37 was also verified by MST with a His tag-specific NT-674 dye labeling LiaX, yielding a K_d similar to full-length protein (5.268 ± 1.141 μM) (*SI Appendix*, Fig. S10). To determine if the binding of the N terminus of LiaX to AMPs is largely charge mediated, we tested an active form of dermcidin (DCD-1L), a membrane-acting anionic AMP that is expressed in human eccrine sweat glands. DCD-1L has broad-spectrum antimicrobial activity, including against *E. faecalis*, with a mechanism of action predicted to be distinct from that of cationic AMPs (23, 24). We confirmed that DCD-1L (50 μg/mL) was active against OG1RF and S613 (*SI Appendix*, Fig. S11). However, in contrast to LL-37, the N-terminal domain of LiaX exhibited no detectable binding affinity to DCD-1L, even at high concentrations (1,000 μM) (*SI Appendix*, Fig. S10 and Table S4). To determine if

a reduction in the cationic charge of LL-37 (+5.9) would impact binding, we tested neutral (substituting alanine and lysine for serine) and charge reversed (substituting some aspartate or arginine residues for lysine or glutamate, net charge −6.1) mutants of LL-37. The binding affinity of the N-terminal domain of LiaX to neutral LL-37 decreased by ~10-fold, with no binding observed to charge reversed LL-37 (*SI Appendix*, Fig. S10 and Table S4). These findings confirm that LiaX, specifically the N-terminal domain, binds DAP and cationic AMPs and that charge likely plays an important role in this interaction.

Protection by LiaX against DAP Is Dependent on a Viable LiaFSR System. Since LiaX binds DAP with high affinity, we postulated that releasing LiaX into the environment is a bacterial strategy to prevent DAP or AMPs from reaching the CM. Thus, we performed a modified spent media assay with MIC determinations that explored the ability of supernatants from DAP-R strains (with excess LiaX) to protect DAP-S strains against DAP. The DAP MIC of the DAP-S clinical isolate S613 increased when grown in the presence of supernatants derived from DAP-R R712 (Fig. 4*A*). Of note, R712 constitutively releases higher amounts of LiaX into the medium than S613 in both the presence and absence of DAP (*SI Appendix*, Fig. S6). Supernatants collected from R712 at late exponential phase yielded maximum protection to S613 relative to those harvested from earlier growth phases (*SI Appendix*, Fig. S12). This implies that higher extracellular accumulation of LiaX by late exponential phase correlates with increased protection. No change in the DAP MIC was observed when OG1RF was exposed to supernatants from OG1RFΔ*liaX* (Fig. 4*A*), confirming that LiaX must be present in the environment for protection. The DAP MIC of DAP-S OG1RF increased in the presence of supernatants from DAP-R OG1RF*liaX*289* (which secretes the N-terminal domain of LiaX), indicating that the N terminus is sufficient to mediate protection (Fig. 4*A*). We then investigated if exogenous addition of purified LiaX or the N terminus alone can protect DAP-S strains. Addition of 50 nM N-terminal LiaX was enough to increase the DAP MIC of OG1RF and S613 over 8-fold (Fig. 4*B*). Full-length LiaX was less potent, with a 2- to 3-fold increase in the DAP MICs. Addition of a range of 1 to 100 nM N-terminal LiaX yielded a high level of protection to OG1RF in a concentration-dependent manner, with the full-length LiaX having a less potent effect even at 200 nM (Fig. 4*C*). Of note, LiaX and its N terminus at their functional concentrations had no impact on the growth of *E. faecalis* (*SI Appendix*, Fig. S13). Furthermore, the N terminus of LiaX (and to a lesser extent, full-length LiaX) protected OG1RF and S613 from LL-37–mediated killing (*SI Appendix*, Fig. S14) in a concentration-dependent manner (*SI Appendix*, Fig. S14*B*).

To assess if the LiaX-mediated protection against DAP was due to direct binding and titration of the antibiotic in the environment or alternatively, through activation of an specific enterococcal signaling network (i.e., LiaFSR), we determined the DAP MIC of DAP-S *Staphylococcus aureus* ATCC29213 (DAP MIC of 0.5 μg/mL) in the presence of supernatants from OG1RF*liaX*289* (Fig. 4*A*) and with the addition of exogenous LiaX or the N terminus of LiaX (Fig. 4*B*). The DAP MIC did not change under any condition, suggesting that the LiaX-mediated effect is specific to *E. faecalis* and that LiaX does not merely sequester DAP to prevent it from binding to the CM. Furthermore, we examined whether the LiaX-protective effect relied on an active LiaFSR system by testing changes on DAP MICs of OG1RF lacking *liaR* using supernatants from OG1RF*liaX*289* and after addition of exogenous LiaX or N-terminal LiaX. The supernatant of OG1RF*liaX*289* (Fig. 4*A*) or the addition of LiaX or N-terminal LiaX (Fig. 4*B*) did not protect OG1RFΔ*liaR* against DAP. Moreover, LiaX and the N terminus of LiaX did not protect OG1RFΔ*liaR* from LL-37–mediated killing (*SI Appendix*, Fig. S14*A*). Thus, we conclude that the mechanism of
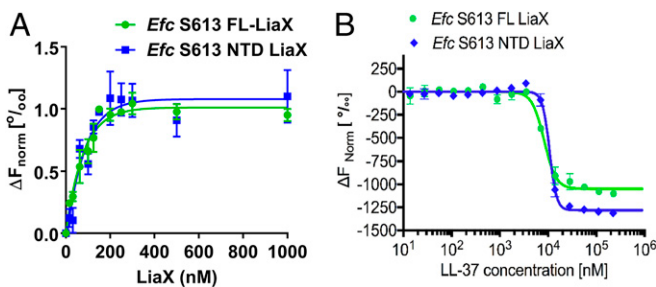

Fig. 3. LiaX and the N terminus of LiaX can bind antimicrobial molecules with high affinity. (*A*) Fluorescence spectroscopy measuring full-length LiaX (FL-LiaX) or N-terminal domain of LiaX (NTD) and DAP binding affinity using the intrinsic fluorescence of DAP (at 465 nm) and increasing concentrations of LiaX or the N terminus of LiaX in the presence of 1 mM Ca^{2+}. (*B*) MST measuring LiaX or the N terminus of LiaX and LL-37 binding affinity in the presence of increasing concentrations of fluorescein-labeled LiaX. Statistics were performed on data from 3 independent experiments.
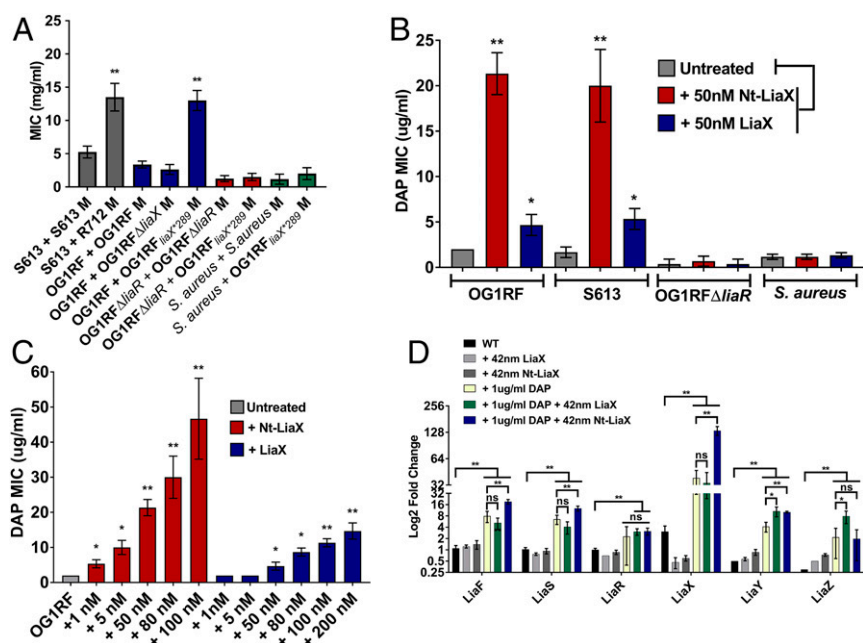
Fig. 4. Extracellular LiaX protects DAP-S strains from DAP attack by activating the LiaFSR stress response. (*A*) Spent medium assay, with DAP MIC for DAP-S strains (first listed strain) determined in the presence of medium from exponential growth of DAP-R strains (denoted M). Spent media from DAP-R strains protect DAP-S *E. faecalis* strains from DAP attack in an LiaR-dependent manner. MIC was measured for each condition in 3 independent experiments with 3 replicates each, and statistics were calculated by 1-way ANOVA. **P < 0.001. (*B*) DAP MIC determination for DAP-S strains by broth microdilution grown with exogenous LiaX or N-terminal LiaX at 50 nM supplemented in the media. Data are an average of 3 experiments with statistics calculated by a 1-way ANOVA. *P < 0.01, **P < 0.001. (*C*) DAP MIC determination of OG1RF by broth microdilution in the presence of increasing concentrations of LiaX or the N terminus of LiaX. Data are an average of 3 experiments with statistics calculated by a 1-way ANOVA. *P < 0.01, **P < 0.001. (*D*) Quantitative real-time PCR for *liaFSR* and *liaXYZ* expression. Statistics compare expression levels with untreated OG1RF and compare DAP plus LiaX or the N terminus of LiaX conditions with DAP alone calculated by 1-way ANOVA. Addition of LiaX and the N terminus of LiaX in the presence of DAP leads to maximal activation of the LiaFSR cell envelope stress response in OG1RF. Data are shown from 3 experiments with 3 biological replicates each. ns, not significant; WT, wild type. **P < 0.001.

LiaX-mediated protection against antimicrobials requires an intact LiaFSR system.

LiaX-Mediated Activation of LiaFSR Requires the Presence of DAP. To determine if the basis of the mechanism of extracellular protection mediated by LiaX or the N terminus of LiaX was a specific response dependent on the presence of cell envelope stress or a stochastic phenomenon due to production of high levels of LiaX in the cellular environment, we assessed the transcriptional activation of *liaFSR* and *liaXYZ* in the presence of LiaX or its *N*-terminal domain by qRT-PCR. Fig. 4*D* shows that adding 50 nM purified LiaX or the N terminus of LiaX in the media of DAP-S OG1RF had no effect on the levels of transcription of the gene clusters relative to untreated controls. However, when DAP (at subinhibitory concentrations) and purified N terminus of LiaX were added, the *liaFSR* and *liaXYZ* operons were highly up-regulated, correlating with maximal activation of the LiaFSR stress response. This is consistent with our in vitro binding studies (Fig. 3*A* and *SI Appendix*, Fig. S10 and Table S4) that suggest that the majority of LiaX would be bound to DAP under these conditions. Most notably, LiaFSR activation with addition of the N terminus of LiaX plus DAP was significantly higher and more pronounced than that of treatment with DAP alone or DAP with full-length LiaX (Fig. 4*D*).

LiaX Mediates Enhanced Virulence In Vivo Due to Resistance to Host Innate Immunity. Inactivation of the LiaFSR system increases the ability of human innate immune cells to clear both *E. faecalis* and *E. faecium* (16). Our binding studies showed that LiaX binds LL-37 with high affinity (Fig. 4*B* and *SI Appendix*, Fig. S10), which led us to postulate that LiaX may play a role in *E. faecalis* pathogenesis and mediate resistance to other host-derived AMPs. We tested this

hypothesis by using the *C. elegans* infection model (25). Both clinical- (Fig. 5*A*) and laboratory-derived (Fig. 5*B*) DAP-R strains displayed increased virulence as measured by nematode killing compared with their DAP-S parental strains. To determine if the enhanced virulence was mediated by increased resistance to AMPs produced by the innate immune system, we tested the ability of *E. faecalis* to infect nematodes lacking the p38 MAP kinase pathway (Δ*pmk-1*), a key immune pathway that regulates important immune effectors, including CM disrupting AMPs (26). Consistent with our hypothesis, DAP-R strains had no virulence advantage over their DAP-S counterparts when infecting the Δ*pmk-1* worms (Fig. 5 *C* and *D*).

Since the N terminus of LiaX serves as a potent signaling molecule that can interact with AMPs, we hypothesized that supplementing the N terminus of LiaX into the media would modulate virulence of *E. faecalis* in the *C. elegans* model. Indeed, OG1RF and S613 were more virulent on addition of the N terminus of LiaX (Fig. 6) in a dose-dependent manner (*SI Appendix*, Fig. S15*A*). Addition of exogenous N terminus of LiaX did not, however, alter the virulence of OG1RF Δ*liaR* and TM Δ*liaR* (Fig. 6 and *SI Appendix*, Fig. S15*B*). Of note, addition of the N terminus alone was not toxic to the worms (*SI Appendix*, Fig. S15*C*). These results suggest that the N terminus of LiaX contributes to increased virulence in vivo by mediating *E. faecalis* protection against AMPs produced by the innate immune system.

Discussion

We have previously shown that the LiaFSR system regulates DAP and AMP resistance in enterococci (12, 15) by causing major changes in the cell envelope, including alterations of CM phospholipid content and architecture (11, 27). Here, we characterize a protein LiaX, a previously unknown mediator of the CM adaptive
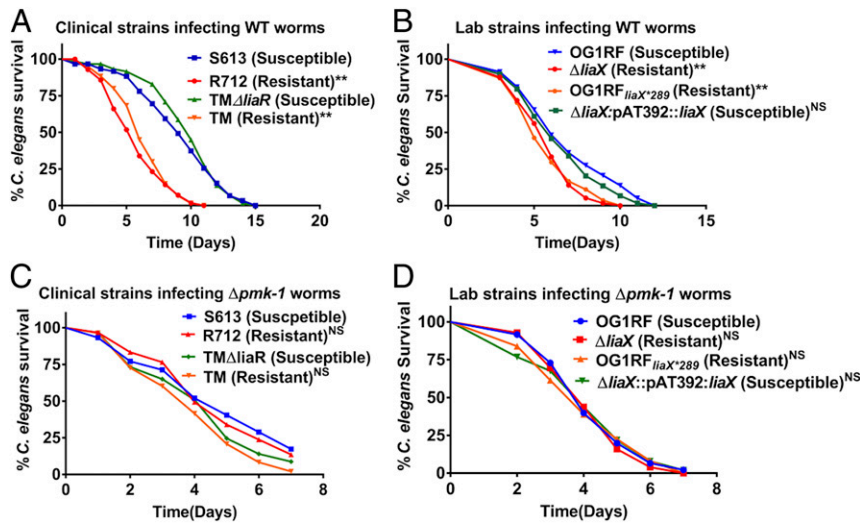
Fig. 5. DAP-R leads to increased virulence in vivo due to innate immune resistance. Lethality of clinical (*A*) or laboratory isolates (*B*) in a wild-type (WT) *C. elegans* infection assay. DAP-R phenotype for each strain is indicated in parentheses. Resistant isolates are more virulent than their DAP-S counterparts. These differences in virulence are abolished when using *C. elegans* harboring a *pmk-1* deletion lacking the primary p38 MAP kinase innate immune pathway (*C* and *D*). The figure represents results from 3 independent experiments with 60 to 90 worms. NS, not significant. **$P < 0.05$.

response to antibiotics and AMPs, as a main modulator of the LiaFSR system. Each domain of LiaX serves a different function. In a DAP-S strain, LiaX is surface exposed, and the C-terminal domain inhibits the LiaFSR system, potentially through the membrane-embedded regulators, LiaF and LiaS (Fig. 7*A*). Thus, DAP-R can evolve via 2 pathways. A C-terminal domain truncation of *liaX* (17) releases the inhibition that this domain has on LiaFSR, leading to CM remodeling and DAP-R. Additionally, mutations in *liaFSR* that occur in clinical settings (11, 13) can activate the system and lead to overexpression and extracellular release of LiaX. When LiaX is overexpressed, both the full-length and N-terminal domains are detected in the extracellular environment. We hypothesize that these 2 forms of LiaX play distinct roles, where the N terminus of LiaX specifically serves as a sentinel to sense and bind antimicrobials to activate the envelope stress response, potentially signaling through other transmembrane components of the LiaFSR system (Fig. 7*B*). In the absence of environmental stressors, the full-length LiaX is able to again bind the membrane-associated regulators, down-regulating gene expression. This would turn "OFF" the stress response in the absence of antimicrobials, allowing anionic phospholipids to localize to the division septum. Both pathways (namely, a C-terminal truncation or secretion of LiaX) lead to CM remodeling, with anionic phospholipids diverted from the septum causing DAP to bind away from its septal targets (11). Each of these strategies converges in clinical resistance, with elimination of the bactericidal activity of DAP and AMPs and also, resulting in increased virulence in vivo. Interestingly, despite lacking transmembrane domains, LPXTG motifs, or a classical secretion signal, LiaX is surface exposed and detected in CM fractions. We thus speculate that the other genes in the operon (*liaYZ*) that encode transmembrane proteins are likely to contribute to the signaling cascade and function as interacting partners of LiaX. Further study is needed to elucidate how LiaX is transferred to the extracellular environment.

CM remodeling can have important consequences on enterococcal virulence in vivo (12). We have previously shown that DAP-R enterococci have an increased ability to survive inside human phagocytes (16). Here, we show that LiaX and specifically, the N-terminal domain bind LL-37 with high affinity. LiaX mediates increased virulence in *C. elegans*, and DAP-R strains have no virulence advantage over DAP-S strains when the innate immune system, responsible for the production of AMPs, is not

functional. The N terminus of LiaX alone is able to increase the virulence of *E. faecalis* (laboratory and clinical isolates) in *C. elegans*. Thus, when mutations in *liaFSR* lead to the extracellular release of the N-terminal domain, AMPs produced by the innate immune system are sensed by LiaX, triggering the CM adaptive response (Fig. 7*B*) and enhancing virulence. Furthermore, LiaFSR mediates bacterial resistance to environmental stressors in natural niches (28). Mutations in *liaR* were shown to enhance VRE gastrointestinal (GI) tract colonization in a mouse model by promoting resistance to lithocholic acid, a bile acid found exclusively in the GI tract (29). Thus, in clinical settings, changes in LiaX could favor enterococcal colonization, resistance against metabolic stressors, and the host innate immunity. Such an adaptive response could also serve as a major selective pressure for developing resistance to DAP during the colonization/
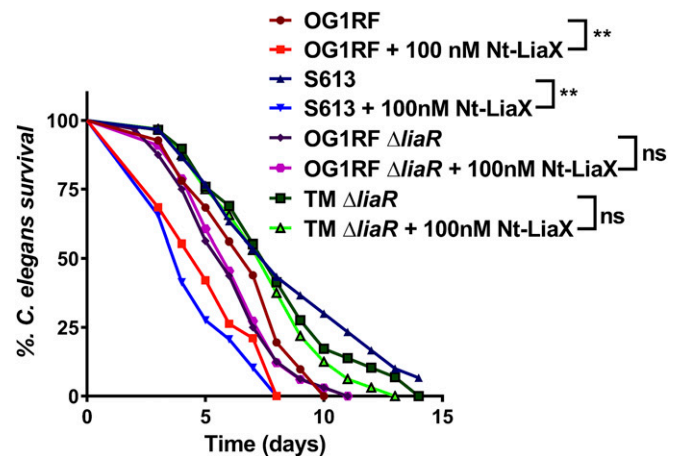

Fig. 6. Addition of N terminus of LiaX leads to increased virulence of DAP-S laboratory (OG1RF) and clinical (S613) strains in *C. elegans*. *C. elegans* infection assay performed with laboratory strain OG1RF or clinical strain S613 and their *liaR* deletion derivatives (OG1RF*ΔliaR* and TM*ΔliaR*, respectively) in the presence or absence of 100 nM purified N-terminal LiaX. Data are represented as average from 3 independent experiments with 60 to 90 nematodes, and significance was calculated with a 1-way ANOVA. ns, not significant. **$P < 0.001$.
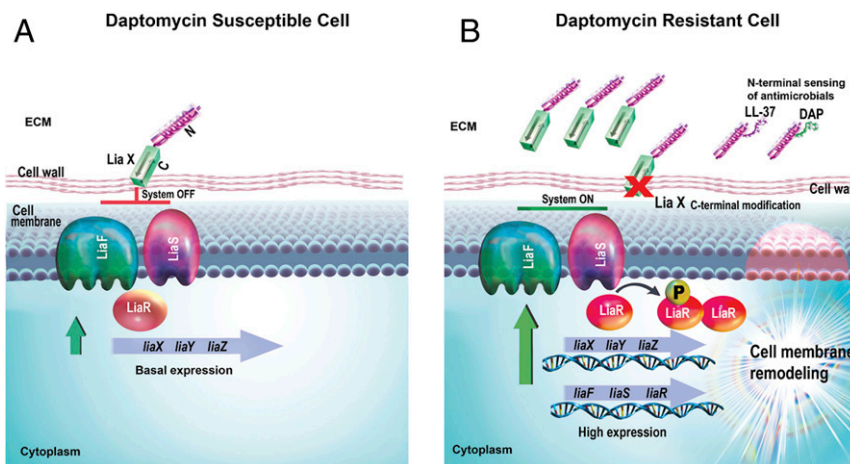
Fig. 7. Mechanistic model of LiaX-mediated DAP-R and antimicrobial peptide resistance. (*A*) The LiaFSR stress response system is in the OFF state in a DAP-S strain under unstressed conditions. LiaX, expressed at basal levels, localizes on the cell surface. The C- and N-terminal domains of LiaX have unique functions. The C-terminal domain likely inhibits the LiaFSR system, while the N-terminal domain faces the extracellular milieu (ECM). The regulators, LiaF and LiaS (histidine kinase sensor), are embedded in the CM. (*B*) A strain becomes DAP resistant through activation of the LiaFSR system due to mutations in *liaFSR* and/ or via a C-terminal truncation of LiaX. LiaX and the N terminus of LiaX are both released into the ECM. In the presence of antimicrobials, like DAP or LL-37, LiaX, in particular the N-terminal domain, serves as a sentinel to bind, activate, and maintain the LiaFSR response. The signaling cascade leads to phosphorylation-dependent oligomerization of the LiaR response regulator, which up-regulates *liaFSR* and *liaXYZ* expression. Both pathways lead to CM remodeling with changes in the architecture of anionic phospholipid microdomains and diversion of DAP away from the division septum.

infection process, jeopardizing the therapeutic efficacy of this antibiotic (30). Moreover, our findings on LiaX mediating resistance to the innate immunity could also explain the fact that some clinical enterococcal strains exhibit resistance to DAP, even in the absence of actual exposure to the antibiotic (5).

In summary, our results highlight the major role of a single protein in orchestrating the cell envelope stress response to antibiotics, influencing membrane adaptation and virulence. This critical function suggests that LiaX could be a potential target for developing antiadaptation molecules that could potentially restore the effectiveness of widely used antimicrobials and enhance innate immunity mechanisms to clear multidrug-resistant infecting bacteria.

Materials and Methods

Microbiology and Molecular Biology Methods. Strains and primers used in this study are listed in *SI Appendix*, Table S1 and S2, respectively. Standard culture media were used for routine strain and plasmid propagation as described in *SI Appendix*, *SI Materials and Methods*. The *liaX* mutants (full deletion, C-terminal truncation) were constructed as described to create an in-frame, nonpolar deletion using the PheS* counterselection system (31, 32) and complemented with pAT392 (33). Recombinant LiaX and the N-terminal domain with a His tag and SUMO tag approach were expressed in pET-Duet vector in *Escherichia coli* BL-21 and purified using a nickel column method (18). For immunoblotting, cell wall extracts were prepared from midexponential-phase cultures using the lysozyme treatment method (34) with membranes isolated by ultracentrifugation at $100,000 \times g$ for 1 h, and supernatants were isolated from the same cultures by 10% trichloroacetic acid (TCA) precipitation. A spent medium assay was used to determine MICs on DAP-S strains in the presence of their own or DAP-R strains spent medium collected at early, mid, and late exponential phases following clinical and laboratory standards institute guidelines. Broth microdilution was performed to determine MICs in the presence of purified LiaX. MICs were read 24 h postinoculation. AMP killing assays were performed in RPMI 1640 media + 5% Luria–Bertani broth for 2 h with a 10^3 inocula or 10 mM sodium phosphate buffer + 100 mM NaCl for 4 h with a 10^6 inocula for 50 μg/mL LL-37 or dermcidin (DCD-1L), respectively (12, 23). Colony-forming unit counts compared survival with the peptide relative to the untreated control. Statistics were calculated between 3 independent experiments with 3 biological replicates with 1-way ANOVA ($P < 0.01$).

Transcriptional Profiling and Quantitative Real-Time PCR. Transcriptome shotgun sequencing comparing DAP-R and DAP-S strains was performed on midexponential-phase cultures in 3 biological replicates with standard RNA

extraction. RNA was quality controlled by bioanalyzer and Nanodrop prior to subjecting to RNA sequencing analysis. DNA Illumina libraries were then sequenced on the HiSeq2000. Complete genome of R712 was sequenced for reference with PacBio. Reads per kilobase million values, read mapping, and alignment (35) for differential expression analysis (36) were performed using a negative binomial fitted model with a Fischer's exact test. qRT-PCR analysis conducted in 3 experiments and 3 biological replicates were performed on exponential-phase cultures grown in the presence or absence of DAP in some instances, as indicated, followed by standard RNA extraction and subsequently, by complementary DNA (cDNA) synthesis and evaluation of gene expression with 5 ng cDNA using SYBR Green. The g*yrB* and *gdhA* housekeeping genes were used for normalization. Differential gene expression was analyzed with 1-way ANOVA ($P < 0.01$).

Lipid Extraction and 2-Dimensional Thin-Layer Chromatography (TLC). Strains were grown to midexponential phase in tryptic soy broth, extracted using a modified Bligh and Dyer method prior to spotting on HPTLC Silica Gel 60 Plates (Millipore), and separated by 2-dimensional TLC (37, 38). Spots developed in $CuSO_4$ + 8% phosphoric acid heated at 180 °C were identified based on previous studies and lipid standards (Avanti Polar Lipids). Relative quantification was performed through ImageJ, with results displayed as an average of 4 biological replicates and statistics calculated by a 1-way ANOVA ($P < 0.05$).

Protein Localization Analysis. Affinity-purified polyclonal anti-rat antibodies raised in house were used for all protein detection assays. Surface exposure and extracellular LiaX were analyzed with an ELISA (39) using an antibody to the N terminus of LiaX performed on exponentially growing whole cells or filter-sterilized and TCA-precipitated supernatants, respectively. Data were compiled from 3 independent experiments with 24 technical replicates for each strain. Two-tailed unpaired *t* test was used for statistics comparing DAP-R and DAP-S pairs in addition to all strains relative to OG1RFΔ*liaX* as negative control. Cell wall extracts and supernatants were normalized using the bicinchoninic assay prior to immunoblotting with the Thermo Fischer iBlot2 and iBind Flex systems. Antibodies to RNA polymerase β-subunit and EbpA, a pilin subunit embedded in the enterococcal cell wall, were used as a cell wall extract quality control.

Microscopy Methods. Anionic phospholipids were visualized by staining with 10-*N*-nonyl acridine orange and fluorescence microscopy as described before (11) with Olympus 1 × 71 or Keyence BX-700 using a cumulative of 3 experiments with 3 biological replicates. Fluorescence intensity was quantified by averaging the relative fluorescence units across cell length for 25 to 50 cells per strain on ImageJ. Immunogold labeling and transmission electron microscopy were performed, as described previously (40), with antibody to

the N terminus of LiaX with anti-rat Immunoglobulin G antibody conjugated to 18-nm gold nanoparticles. Samples with 3 biological replicates were imaged using a JEOL JEM 1400 120-kV microscope.

LiaX and Antimicrobial Molecule Binding Assays. Determination of LiaX binding affinity to DAP, LL-37 variants, and dermcidin was performed with fluorescence spectroscopy or MST (41). For DAP, the excitation was at 365 nm with emission at 465 nm to observe Kyn-13–emitted fluorescence in the presence of increasing LiaX concentrations. MST experiments were performed on Monolith NT.115 using 25% light-emitting diode with LiaX NT-647 labeled (in 0.1 M phosphate buffer, pH 7.4, 0.0027 M potassium chloride, 0.137 M NaCl, and 1 mM Tris [2-carboxyethyl] Phosphine with or without 5% dimethyl sulfoxide) and tested in the presence of increasing LL-37 variant or dermcidin concentrations. Data analysis was performed with Nanotemper software v1.5.41.

***C. elegans* Infection Model.** In order to assess virulence of DAP-R strains relative to their susceptible counterparts, we used a *C. elegans* infection model as previously described (25). Briefly, 60 to 90 synchronized young adult nematodes [wild type or *pmk-1(km25)*] (26) were infected with *E. faecalis* strains on brain heart infusion (BHI) agar containing gentamicin (10 μg/mL). For assays with exogenous LiaX, a modified liquid killing assay was performed (42) by transferring worms to 20% BHI broth, 80% M9W buffer, and the N terminus of LiaX (0.1 to 500 nM). The plates were incubated at 25 °C, and worm death was scored daily. Kaplan–Meier log rank analysis was used to compare survival curves pairwise ($P < 0.05$) calculated from 3 independent experiments.

1. World Health Organization, *Antimicrobial Resistance Global Report on Surveillance* (World Health Organization, Geneva, Switzerland, 2014).
2. L. M. Weiner *et al.*, Antimicrobial-resistant pathogens associated with healthcare-associated infections: Summary of data reported to the national healthcare safety network at the centers for disease control and prevention, 2011-2014. *Infect. Control Hosp. Epidemiol.* **37**, 1288–1301 (2016).
3. C. A. Arias, B. E. Murray, The rise of the Enterococcus: Beyond vancomycin resistance. *Nat. Rev. Microbiol.* **10**, 266–278 (2012).
4. C. A. Arias, G. A. Contreras, B. E. Murray, Management of multidrug-resistant enterococcal infections. *Clin. Microbiol. Infect.* **16**, 555–562 (2010).
5. T. Kelesidis, R. Humphries, D. Z. Uslan, D. A. Pegues, Daptomycin nonsusceptible enterococci: An emerging challenge for clinicians. *Clin. Infect. Dis.* **52**, 228–234 (2011).
6. S. D. Taylor, M. Palmer, The action mechanism of daptomycin. *Bioorg. Med. Chem.* **24**, 6253–6268 (2016).
7. A. Müller *et al.*, Daptomycin inhibits cell envelope synthesis by interfering with fluid membrane microdomains. *Proc. Natl. Acad. Sci. U.S.A.* **113**, E7077–E7086 (2016).
8. S. K. Straus, R. E. Hancock, Mode of action of the new antibiotic for gram-positive pathogens daptomycin: Comparison with cationic antimicrobial peptides and lipopeptides. *Biochim. Biophys. Acta* **1758**, 1215–1223 (2006).
9. R. E. Hancock, G. Diamond, The role of cationic antimicrobial peptides in innate host defences. *Trends Microbiol.* **8**, 402–410 (2000).
10. N. N. Mishra *et al.*, Daptomycin resistance in enterococci is associated with distinct alterations of cell membrane phospholipid content. *PLoS One* **7**, e43958 (2012).
11. T. T. Tran *et al.*, Daptomycin-resistant Enterococcus faecalis diverts the antibiotic molecule from the division septum and remodels cell membrane phospholipids. *MBio* **4**, e00281-13 (2013).
12. J. Reyes *et al.*, A liaR deletion restores susceptibility to daptomycin and antimicrobial peptides in multidrug-resistant Enterococcus faecalis. *J. Infect. Dis.* **211**, 1317–1325 (2015).
13. C. A. Arias *et al.*, Genetic basis for in vivo daptomycin resistance in enterococci. *N. Engl. J. Med.* **365**, 892–900 (2011).
14. T. T. Tran, J. M. Munita, C. A. Arias, Mechanisms of drug resistance: Daptomycin resistance. *Ann. N. Y. Acad. Sci.* **1354**, 32–53 (2015).
15. D. Panesso *et al.*, Deletion of liaR reverses daptomycin resistance in Enterococcus faecium independent of the genetic background. *Antimicrob. Agents Chemother.* **59**, 7327–7334 (2015).
16. S. Rincon *et al.*, Disrupting membrane adaptation restores in vivo efficacy of antibiotics against multidrug-resistant enterococci and potentiates killing by human neutrophils. *J Infect Dis.* **220**, 494–504 (2019).
17. C. Miller *et al.*, Adaptation of Enterococcus faecalis to daptomycin reveals an ordered progression to resistance. *Antimicrob. Agents Chemother.* **57**, 5373–5383 (2013).
18. M. Davlieva *et al.*, A variable DNA recognition site organization establishes the LiaR-mediated cell envelope stress response of enterococci to daptomycin. *Nucleic Acids Res.* **43**, 4758–4773 (2015).
19. N. Joly *et al.*, Managing membrane stress: The phage shock protein (Psp) response, from molecular mechanisms to physiology. *FEMS Microbiol. Rev.* **34**, 797–827 (2010).
20. S. Kamilla, V. Jain, Mycobacteriophage D29 holin C-terminal region functionally assists in holin aggregation and bacterial cell death. *FEBS J.* **283**, 173–190 (2016).
21. M. Shahmiri *et al.*, Membrane core-specific antimicrobial action of cathelicidin LL-37 peptide switches between pore and nanofibre formation. *Sci. Rep.* **6**, 38184 (2016).
22. A. S. Bayer *et al.*, Frequency and distribution of single-nucleotide polymorphisms within mprF in methicillin-resistant Staphylococcus aureus clinical isolates and their role in cross-resistance to daptomycin and host defense antimicrobial peptides. *Antimicrob. Agents Chemother.* **59**, 4930–4937 (2015).
23. B. Schittek *et al.*, Dermcidin: A novel human antibiotic peptide secreted by sweat glands. *Nat. Immunol.* **2**, 1133–1137 (2001).
24. I. Senyürek *et al.*, Dermcidin-derived peptides show a different mode of action than the cathelicidin LL-37 against Staphylococcus aureus. *Antimicrob. Agents Chemother.* **53**, 2499–2509 (2009).
25. D. A. Garsin *et al.*, A simple model host for identifying Gram-positive virulence factors. *Proc. Natl. Acad. Sci. U.S.A.* **98**, 10892–10897 (2001).
26. D. H. Kim *et al.*, A conserved p38 MAP kinase pathway in Caenorhabditis elegans innate immunity. *Science* **297**, 623–626 (2002).
27. L. Diaz *et al.*, Whole-genome analyses of Enterococcus faecium isolates with diverse daptomycin MICs. *Antimicrob. Agents Chemother.* **58**, 4527–4534 (2014).
28. S. Jordan, M. I. Hutchings, T. Mascher, Cell envelope stress response in Gram-positive bacteria. *FEMS Microbiol. Rev.* **32**, 107–146 (2008).
29. P. T. McKenney *et al.*, Intestinal bile acids induce a morphotype switch in vancomycin-resistant Enterococcus that facilitates intestinal colonization. *Cell Host Microbe* **25**, 695–705.e5 (2019).
30. T. Kelesidis, R. Humphries, D. Z. Uslan, D. Pegues, De novo daptomycin-nonsusceptible enterococcal infections. *Emerg. Infect. Dis.* **18**, 674–676 (2012).
31. C. J. Kristich, J. R. Chandler, G. M. Dunny, Development of a host-genotype-independent counterselectable marker and a high-frequency conjugative delivery system and their use in genetic analysis of Enterococcus faecalis. *Plasmid* **57**, 131–144 (2007).
32. D. Panesso *et al.*, The hylEfm gene in pHylEfm of Enterococcus faecium is not required in pathogenesis of murine peritonitis. *BMC Microbiol.* **11**, 20 (2011).
33. M. Arthur, F. Depardieu, H. A. Snaith, P. E. Reynolds, P. Courvalin, Contribution of VanY D,D-carboxypeptidase to glycopeptide resistance in Enterococcus faecalis by hydrolysis of peptidoglycan precursors. *Antimicrob. Agents Chemother.* **38**, 1899–1903 (1994).
34. S. Brinster, S. Furlan, P. Serror, C-terminal WxL domain mediates cell wall binding in Enterococcus faecalis and other gram-positive bacteria. *J. Bacteriol.* **189**, 1244–1253 (2007).
35. T. Magoc, D. Wood, S. L. Salzberg, EDGE-pro: Estimated degree of gene expression in Prokaryotic genomes. *Evol. Bioinform. Online* **9**, 127–136 (2013).
36. M. I. Love, W. Huber, S. Anders, Moderated estimation of fold change and dispersion for RNA-seq data with DESeq2. *Genome Biol.* **15**, 550 (2014).
37. Y. Bao *et al.*, Role of mprF1 and mprF2 in the pathogenicity of Enterococcus faecalis. *PLoS One* **7**, e38458 (2012).
38. S. Klein *et al.*, Adaptation of Pseudomonas aeruginosa to various conditions includes tRNA-dependent formation of alanyl-phosphatidylglycerol. *Mol. Microbiol.* **71**, 551–565 (2009).
39. S. R. Nallapareddy, G. M. Weinstock, B. E. Murray, Clinical isolates of Enterococcus faecium exhibit strain-specific collagen binding mediated by Acm, a new member of the MSCRAMM family. *Mol. Microbiol.* **47**, 1733–1747 (2003).
40. A. Swierczynski, H. Ton-That, Type III pilus of corynebacteria: Pilus length is determined by the level of its major pilin subunit. *J. Bacteriol.* **188**, 6318–6325 (2006).
41. M. Jerabek-Willemsen, C. J. Wienken, D. Braun, P. Baaske, S. Duhr, Molecular interaction studies using microscale thermophoresis. *Assay Drug Dev. Technol.* **9**, 342–353 (2011).
42. S. Rincon *et al.*, Disrupting membrane adaptation restores in vivo efficacy of antibiotics against multidrug-resistant enterococci and potentiates killing by human neutrophils. *J. Infect. Dis.* **220**, 494–504 (2019).